# Optical vortex arrays from smectic liquid crystals

**Baeksik Son,[1,8] Sejeong Kim,[2,8] Yun Ho Kim,[3] K. Käläntär,[4] Hwi-Min Kim,[2] Hyeon-Su Jeong,[1] Siyoung Q. Choi,[5] Jonghwa Shin,[6] Hee-Tae Jung,[1,9] and Yong-Hee Lee[2,7,*]**

[1]*Department of Chemical and Biomolecular Engineering, Korea Advanced Institute of Science and Technology, Daejeon 305-701, South Korea*
[2]*Department of Physics, Korea Advanced Institute of Science and Technology, Daejeon 305-701, South Korea*
[3]*Advanced Functional Materials Research Group, Korea Research Institute of Chemical Technology, Daejeon 305-600, South Korea*
[4]*Global Optical Solutions, Tokyo 193-0832, Japan*
[5]*Information and Electrical Research Institute, Korea Advanced Institute of Science and Technology, Daejeon 305-701, South Korea*
[6]*Department of Materials Science and Engineering, Korea Advanced Institute of Science and Technology, Daejeon 305-701, South Korea*
[7]*Graduate School of Nanoscience and Technology (WCU), Korea Advanced Institute of Science and Technology, Daejeon 305-701, South Korea*
[8]*These authors contributed equally to this work.*
[9]*heetae@kaist.ac.kr*
[*]*yhlee@kaist.ac.kr*

**Abstract:** We demonstrate large-area, closely-packed optical vortex arrays using self-assembled defects in smectic liquid crystals. Self-assembled smectic liquid crystals in a three-dimensional torus structure are called focal conic domains. Each FCD, having a micro-scale feature size, produces an optical vortex with consistent topological charge of 2. The spiral profile in the interferometry confirms the formation of an optical vortex, which is predicted by Jones matrix calculations.



**OCIS codes:** (050.4865) Optical vortices; (230.3720) Liquid-crystal devices.

## References and links

1. X. Cai, J. Wang, M. J. Strain, B. Johnson-Morris, J. Zhu, M. Sorel, J. L. O'Brien, M. G. Thompson, and S. Yu, "Integrated compact optical vortex beam emitters," Science **338**(6105), 363–366 (2012).
2. E. Brasselet and C. Loussert, "Electrically controlled topological defects in liquid crystals as tunable spin-orbit encoders for photons," Opt. Lett. **36**(5), 719–721 (2011).
3. M. Totzeck and H. J. Tiziani, "Phase-singularities in 2D diffraction fields and interference microscopy," **138**, 365-382 (1997).
4. V. G. Shvedov, A. V. Rode, Y. V. Izdebskaya, A. S. Desyatnikov, W. Krolikowski, and Y. S. Kivshar, "Giant optical manipulation," Phys. Rev. Lett. **105**(11), 118103 (2010).
5. E. Nagali, F. Sciarrino, F. De Martini, B. Piccirillo, E. Karimi, L. Marrucci, and E. Santamato, "Polarization control of single photon quantum orbital angular momentum states," Opt. Express **17**(21), 18745–18759 (2009).
6. G. Foo, D. M. Palacios, and G. A. Swartzlander, Jr., "Optical vortex coronagraph," Opt. Lett. **30**(24), 3308–3310 (2005).
7. D. Voloschenko and O. D. Lavrentovich, "Optical vortices generated by dislocations in a cholesteric liquid crystal," Opt. Lett. **25**(5), 317–319 (2000).
8. L. Marrucci, C. Manzo, and D. Paparo, "Optical spin-to-orbital angular momentum conversion in inhomogeneous anisotropic media," Phys. Rev. Lett. **96**(16), 163905 (2006).
9. N. Yu, P. Genevet, M. A. Kats, F. Aieta, J.-P. Tetienne, F. Capasso, and Z. Gaburro, "Light propagation with phase discontinuities: Generalized laws of reflection and refraction," Science **334**(6054), 333–337 (2011).
10. E. Brasselet, N. Murazawa, H. Misawa, and S. Juodkazis, "Optical vortices from liquid crystal droplets," Phys. Rev. Lett. **103**(10), 103903 (2009).
11. C. Loussert, U. Delabre, and E. Brasselet, "Manipulating the Orbital Angular Momentum of Light at The Micron Scale with Nematic Disclinations in a Liquid Crystal Film," Phys. Rev. Lett. **111**(3), 037802 (2013).
12. H. T. Dai, Y. J. Liu, D. Luo, and X. W. Sun, "Propagation properties of an optical vortex carried by an Airy beam: experimental implementation," Opt. Lett. **36**(9), 1617–1619 (2011).
13. H. T. Dai, Y. J. Liu, D. Luo, and X. W. Sun, "Propagation dynamics of an optical vortex imposed on an Airy beam," Opt. Lett. **35**(23), 4075–4077 (2010).
14. E. Brasselet, "Spin-orbit optical cross-phase-modulation," Phys. Rev. A **82**(6), 063836 (2010).

#204639 - $15.00 USD Received 13 Jan 2014; revised 12 Feb 2014; accepted 12 Feb 2014; published 20 Feb 2014

15. K. Ladavac and D. Grier, "Microoptomechanical pumps assembled and driven by holographic optical vortex arrays," Opt. Express **12**(6), 1144–1149 (2004).
16. C. R. Doerr and L. L. Buhl, "Circular grating coupler for creating focused azimuthally and radially polarized beams," Opt. Lett. **36**(7), 1209–1211 (2011).
17. A. Mair, A. Vaziri, G. Weihs, and A. Zeilinger, "Entanglement of the orbital angular momentum states of photons," Nature **412**(6844), 313–316 (2001).
18. D. P. Ghai, S. Vyas, P. Senthilkumaran, and R. S. Sirohi, "Vortex lattice generation using interferometric techniques based on lateral shearing," Opt. Commun. **282**(14), 2692–2698 (2009).
19. E. Brasselet, M. Malinauskas, A. Žukauskas, and S. Juodkazis, "Photopolymerized microscopic vortex beam generators: Precise delivery of optical orbital angular momentum," Appl. Phys. Lett. **97**(21), 211108 (2010).
20. E. Brasselet, A. Royon, and L. Canioni, "Dense arrays of microscopic optical vortex generators from femtosecond direct laser writing of radial birefringence in glass," Appl. Phys. Lett. **100**(18), 181901 (2012).
21. B. Yang and E. Brasselet, "Arbitrary vortex arrays realized from optical winding of frustrated chiral liquid crystals," J. Opt. **15**(4), 044021 (2013).
22. E. Brasselet, "Tunable optical vortex arrays from a single nematic topological defect," Phys. Rev. Lett. **108**(8), 087801 (2012).
23. R. Barboza, U. Bortolozzo, G. Assanto, E. Vidal-Henriquez, M. G. Clerc, and S. Residori, "Harnessing optical vortex lattices in nematic liquid crystals," Phys. Rev. Lett. **111**(9), 093902 (2013).
24. Y. H. Kim, D. K. Yoon, M. C. Choi, H. S. Jeong, M. W. Kim, O. D. Lavrentovich, and H.-T. Jung, "Confined self-assembly of toric focal conic domains (the effects of confined geometry on the feature size of toric focal conic domains)," Langmuir **25**(3), 1685–1691 (2009).
25. Y. H. Kim, D. K. Yoon, H. S. Jeong, O. D. Lavrentovich, and H.-T. Jung, "Smectic liquid crystal defects for self-assembling of building blocks and their lithographic applications," Adv. Funct. Mater. **21**(4), 610–627 (2011).
26. F. Li, W. J. Doane, and A. Jákli, "Magical Smectic Liquid Crystal Tube: Simple Illustration of Mechanical, Optical and Magnetic Properties of Smectic Liquid Crystals," Jpn. J. Appl. Phys. **45**(3A), 1714–1718 (2006).
27. C. Meyer, L. Le Cunff, M. Belloul, and G. Foyart, "Focal Conic Stacking in Smectic A Liquid Crystals: Smectic Flower and Apollonius Tiling," Materials **2**(2), 499–513 (2009).
28. D. Mawet, E. Serabyn, K. Liewer, Ch. Hanot, S. McEldowney, D. Shemo, and N. O'Brien, "Optical vectorial vortex coronagraphs using liquid crystal polymers: theory, manufacturing and laboratory demonstration," Opt. Express **17**(3), 1902–1918 (2009).

## 1. Introduction

Creating microscopic optical vortices has been one of the interesting issues in the field of integrated optics [1,2]. Optical vortices can be used to develop new methods for high-resolution microscopy [3], optical manipulation [4], quantum computing [5], and astronomical imaging [6]. Several techniques of single optical vortex generation have been devised thus far [7–14], at the same time, the need for an array of optical vortices has also been increasing for applications such as opto-mechanical pump drives [15], multichannel optical communications [16], and quantum information [17]. Recently, multiple optical vortices have been demonstrated by utilizing diverse methods including interferometry [18], electron-beam lithography [1], photo-polymerization [19], and direct laser writing of radial birefringence [20]. Among many strategies, the use of liquid crystals (LCs) has been frequently adopted to generate optical vortex arrays on the bases of its advantages associated with the ability to achieve rapid and simple stabilization of molecular ordering and structure [7,20]. Arrays of microscopic optical vortex generators using cholesteric [7,21] or nematic [22,23] LCs have also been successfully realized recently.

In this study, we demonstrate a method to produce closely-packed, highly ordered optical vortex arrays over a large area using self-assembled smectic LC defects, called focal conic domains (FCDs) [24,25]. Each FCD, having a micro-scale (10-35 μm) feature size, generate an optical vortex with consistent topological charge of 2. The spiral profile in the interferometry confirms the formation of an optical vortex, which is predicted by Jones matrix calculations. This study is the first to report a formation of an optical vortex array with a self-assembled smectic LC phase. The proposed method is simple, fast and able to generate micro-scale vortices.

## 2. Sample preparation and theoretical calculations

The smectic LC layer produces uniform FCD structures by self-assembly, which have circular shape and dimple-like outer surfaces. In this process, a simple rod-like smectic LC, 4'-octyloxy-biphenyl-4-carboxylic acid 2-methylbutyl ester, containing a rigid aromatic group

#204639 - $15.00 USD Received 13 Jan 2014; revised 12 Feb 2014; accepted 12 Feb 2014; published 20 Feb 2014

and alkyl tails, is used [26]. In order to achieve random planar anchoring of the smectic LC on a quartz glass substrate, a uniform polyethyleneimine (PEI) layer of 10 nm thickness is spin-coated onto the glass. Following deposition of the crystalline LC material, the substrate is heated to temperature exceeding 65 °C (corresponding to the isotropic phase of the LC) and then cooled at a rate of −5°C/min to form the smectic A phase. This procedure consistently afforded highly ordered, hexagonal patterned FCDs substrate.

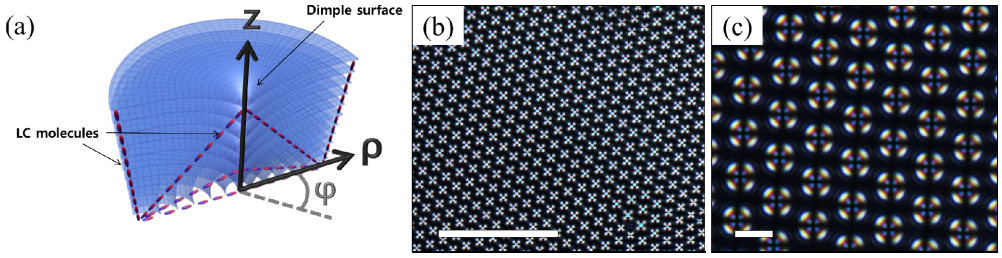


Fig. 1. (a) Three-dimensional schematic view of the FCD. (b) Optical microscope image of the hexagonal FCD arrays between crossed linear polarizers (scale bar is 100 μm) and (c) magnified image (scale bar is 10 μm).

The LC molecular alignment inside the FCD is illustrated in Fig. 1(a). Self-assembled FCDs have a varying director field along the $\rho$ and $z$ directions. The director is the distinguishing characteristic of the liquid crystalline state to point a local LC molecule orientation. LC molecules close to the surface of the PEI coated substrate are preferentially aligned parallel to the surface, while those at the air-LC interface tend to align perpendicular to the interface. Figure 1(b) shows a polarized optical microscopy (POM) image of the FCD domains of smectic LCs on a flat PEI-coated slide glass substrate and reveals the formation of highly ordered FCDs over a large area of hundreds of square-micrometers, with more than ~1,000 FCDs. Each small circular domain corresponds to a single FCD. Close inspection of the POM images, presented in Fig. 1(c), of the film formed by the LC materials discloses that the FCDs have identical sizes with 8 μm diameters and exist as a hexagonal array.

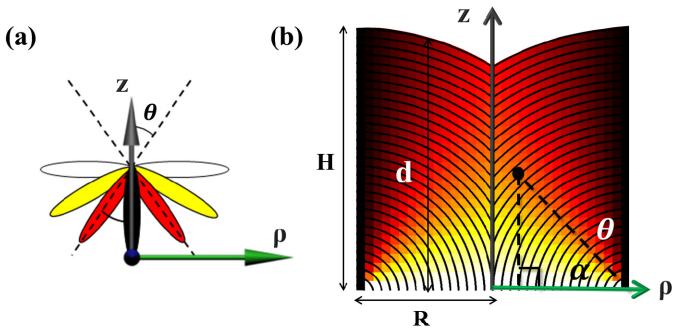


Fig. 2. (a) The LC molecular director is represented by the polar angle $\theta$ and mapped in colors. (b) A schematically drawn cross-section of a FCD with structural parameters. R and H are fixed constants that correspond to the radius and height of the FCD, respectively. The thickness of the FCD, which depends on $\rho$, is defined as $d$. The black dot and the dashed line is drawn to derive Eq. (1).

Schematic illustrations of the FCD with geometric parameters are portrayed in Fig. 2 [27]. The orientation of the LC molecular director, $\theta(\rho, z)$, is represented in Fig. 2(a). $\theta$ at the specific coordinate, $(\rho, z)$, can be derived by drawing a triangle as in Fig. 2(b). By calculating $\tan\alpha$, one can get Eq. (1).

#204639 - $15.00 USD Received 13 Jan 2014; revised 12 Feb 2014; accepted 12 Feb 2014; published 20 Feb 2014

$$\theta(\rho,z)=\frac{\pi}{2}-\tan^{-1}\left(\frac{z}{R-\rho}\right) \tag{1}$$

LC molecules with different $\theta$ are depicted by different colors, which are also applied to the director field distribution mapping in Fig. 2(b). Here, we defined several parameters for mathematical use. There are two constants, $R$ and $H$, which indicate the outermost radius and the height at the boundary of the FCD, respectively. The radius dependent variable $d$ indicates the curved height resulting from the dimple-like outer surface and can be described by $d=\sqrt{H^2-(\mathrm{R}-\rho)^2}$ . The total phase retardation $\Delta\Phi$ , between the extraordinary and ordinary light is defined as Eq. (2) and Eq. (3) at the output beam. $n_{eff}$ represents the effective refractive index when the director makes angle $\theta$ to z axis. $n_{\|}$ and $n_{\perp}$ are refractive indices along and perpendicular to the LC director which corresponds to 1.67 and 1.53 respectively [26]. The Jones matrix for an axially symmetric birefringent material with a topological charge $m$, is represented in Eq. (4) [28]. Finally, the intensity pattern observed when placing the sample between crossed linear polarizers is expressed by Eq. (5). The equation well explains the experiment results in Fig. 3 when the topological charge $m$ is 2.

$$\Delta\Phi(\rho)=\frac{2\pi}{\lambda}\int_0^d[n_{eff}(\rho,z)-n_{\perp}]\mathrm{dz} \tag{2}$$

$$n_{eff}(\rho,z)=\frac{n_{\|}n_{\perp}}{[n_{\|}^2\cos^2\theta(\rho,z)+n_{\perp}^2\sin^2\theta(\rho,z)]^{1/2}} \tag{3}$$

$$J(\rho,\varphi)=-i\sin\frac{\Delta\Phi(\rho)}{2}\begin{bmatrix}\cos m\varphi & \sin m\varphi\\ \sin m\varphi & -\cos m\varphi\end{bmatrix}+\cos\frac{\Delta\Phi(\rho)}{2}\begin{bmatrix}1 & 0\\ 0 & 1\end{bmatrix} \tag{4}$$

$$I_{out}(\rho,\varphi)=\left|\Psi_{out}(\rho,\varphi)\right|^2=\sin^2(m\varphi)\sin^2\left(\frac{\Delta\Phi(\rho)}{2}\right) \tag{5}$$

## 3. Experimental results

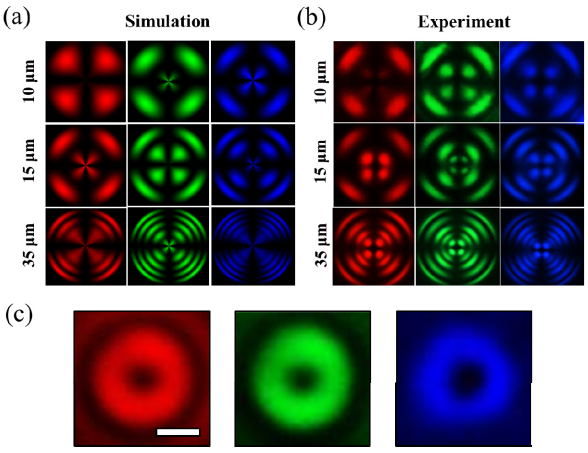


Fig. 3. (a) Numerically calculated intensity profiles between vertically crossed polarizers in different FCD size and input wavelength. (b) Experimental results of intensity profiles are in good agreement with simulation results. (c) Optical microscope images of doughnut intensity beam profiles with different input wavelength. Input light is unpolarized. (Scale bar is 2 μm.)

#204639 - $15.00 USD Received 13 Jan 2014; revised 12 Feb 2014; accepted 12 Feb 2014; published 20 Feb 2014

Intensity patterns of the light transmission between crossed linear polarizers are observed with different FCD size and input beam wavelength, as seen in Fig. 3(a). The simulated results show that the number of four-fold symmetry fringes increases as the size becomes larger and the wavelength becomes shorter. Experimental patterns in Fig. 3(b) exhibit similar behaviors with the simulation for different input wavelengths and FCD sizes. The dark core observed at the beam center, as in Fig. 3(c), is another characteristic of an optical vortex. The optical microscope image of the optical vortex with un-polarized input light has a doughnut shaped intensity profile.

Thus far, the analysis using the Jones matrix has been presented with linearly polarized input beams. However, a calculation with a circularly polarized basis shows direct evidence for the optical vortex. For the left-handed circularly polarized (LHCP) input beam, for example, some portion of light is transformed into a right-handed circularly polarized (RHCP) output beam carrying local optical vortex phase term $e^{im\varphi}$, while the other portion maintains its original polarization as in Eq. (6). From the equation, we can estimate the vortex generation efficiency by averaging the coefficient of the vortex phase-containing term, i.e. $\sin^2\frac{\Delta\Phi}{2}$, over the whole output beam cross-section area. The optical vortex generation efficiency is 0.45 for 8 μm-sized FCDs and 633 nm input beam. The efficiency converges to 0.5 as the diameter increases or the input wavelength decreases.

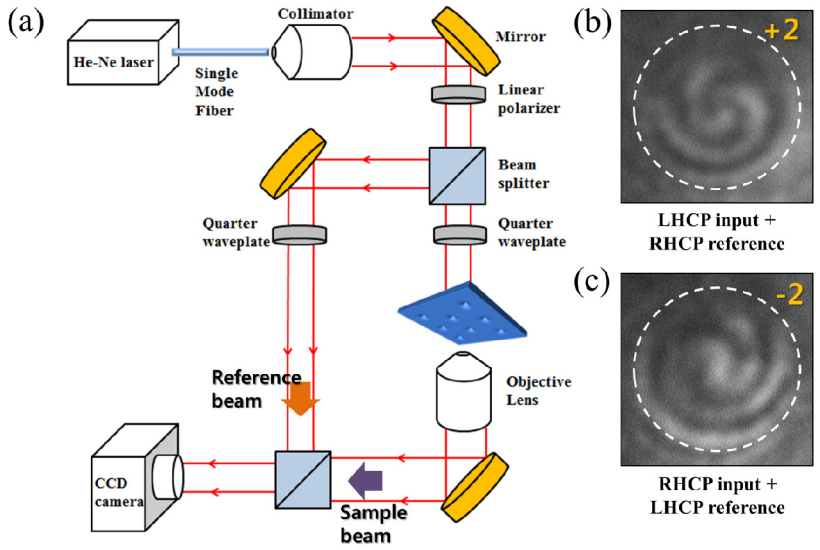


Fig. 4. (a) The experimental setup. LHCP or RHCP gaussian reference beam interferes with the sample beam and projected onto the visible camera. Spiral fringes in the interference pattern is shown when the input beam is (b) the LHCP light and (c) the RHCP light, respectively.

$$\Psi_{out} = J(\rho,\varphi)\begin{bmatrix}1\\ i\end{bmatrix} = \frac{1}{\sqrt{2}}\left(-ie^{im\varphi}\sin\frac{\Delta\Phi(\rho)}{2}\begin{bmatrix}1\\ -i\end{bmatrix} + \cos\frac{\Delta\Phi(\rho)}{2}\begin{bmatrix}1\\ i\end{bmatrix}\right) \quad (6)$$

Theoretical prediction for optical vortex generation from Eq. (6) is confirmed by experimental setup shown in Fig. 4(a). To investigate the phase structure from the FCD, the co-propagating circularly polarized reference beam interferes with the sample beam to form m-armed profiles [2].

The LHCP (RHCP) input beam is converted into an RHCP (LHCP) beam, thus it makes spiral fringes when it interferes with the RHCP (LHCP) reference beam while no spiral fringes appear with the LHCP (RHCP) reference beam. Figure 4(b) and Fig. 4(c) show two-

#204639 - $15.00 USD Received 13 Jan 2014; revised 12 Feb 2014; accepted 12 Feb 2014; published 20 Feb 2014

armed spiral fringes with opposite direction which correspond to topological charge of + 2 and −2, respectively.

## 4. Conclusion

In summary, we demonstrate that a self-assembled FCD with intrinsic torus geometry generates an optical vortex of topological charge 2. The formation of the optical vortex was confirmed by the results of a geometric investigation, POM image analysis and the typical interference pattern with spherical-wavefronted reference beam. The array forming self-assembly and self-organization of FCDs can potentially serve as technique for mass production of micro-sized optical vortices. The ability to conveniently fabricate these arrays will have a significant impact on various modern optical technologies, including multiple-mode particle trapping and quantum parallel-computing.

## Acknowledgments

Baesik Son and Sejeong Kim contributed equally to this work. Y.-H.L. acknowledges support provided by National Research Foundation of Korea Grants (2007-0093863, 2009-0087691, 2012-0087691, 2012-00087) and the World Class University (WCU) program (R31-2008-000-10071-0). H.-T.J. acknowledges support by National Research Foundation of Korea Grants (2012 R1A2A1A01003537, 2009-008338) and the World Class University (WCU) program (R32-2008-000-10142-0).

#204639 - $15.00 USD Received 13 Jan 2014; revised 12 Feb 2014; accepted 12 Feb 2014; published 20 Feb 2014